If the chain is composed of $l$ links and $p$ kinematic pairs, then its dof $f$ is given by the difference between its total dof before coupling and the sum of its restrictions, i.e.,

$$f = d_m(l-1) - \sum_{i=1}^{p} r_i \tag{2.12}$$

The above relation can be termed a *generalized Chebyshev-Grübler-Kutzbach* (CGK) formula in that it generalizes the concept involved in parameter $d_m$ above. Conventional CGK formulas usually consider that $d_m$ can attain one of two possible values, 3 for planar and spherical chains and 6 for spatial chains. In the generalized formula, $d_m$ can attain any of the values 2, 3, 4, or 6. Moreover, rather than considering only three subgroups of displacements, we consider all 12 described above, none of which is of dimension five.

As an example of the application of the above formula, we consider the *vise mechanism*, displayed in Fig. 2.14. In that figure, we distinguish three links and three LKPs. The links are the frame 1, the crank 2 and the slider 3, which define three bonds, namely,

$$\mathcal{L}(1,2) = \mathcal{R}(\mathcal{A}), \quad \mathcal{L}(2,3) = \mathcal{H}(\mathcal{A}), \quad \mathcal{L}(3,1) = \mathcal{P}(\mathbf{a})$$

in which $\mathcal{A}$ is the common axis of the R and the H pairs, while $\mathbf{a}$ is the unit vector parallel to $\mathcal{A}$. In this case, it is apparent that all three bonds lie in the $\mathcal{C}$ subgroup, and hence, $d_m = 2$. Moreover, if we number the three joints in the order R, H, P, and notice that the dimension $d_i$ associated with each of the three joints is unity, then $r_i = 1$, for $i = 1, 2, 3$. Application of the generalized CGK formula (2.12) yields

$$f = 2(3-1) - 3 \times 1 = 4 - 3 = 1$$

which is indeed the correct value of the vise dof.

While the generalized CGK formula is more broadly applicable and less error-prone than its conventional counterpart, it is not error-free. Indeed, let us consider the HHHRRH closed chain of Fig. 2.15, first proposed by Hervé (1978). The four H pairs of this figure have distinct pitches.

It is apparent that all links move in parallel planes, and that these planes also translate along their common normal direction. The displacement subgroup containing all possible kinematic bonds of the mechanism under study, of minimum dimension, is thus the Schönflies subgroup $\mathcal{X}(\mathbf{u})$, and hence, $d_m = 4$. Since we have six links and six joints, each of restriction $r_i = d_m - f_i$, for $f_i = 1$ and $i = 1, \ldots, 6$, the dof of the mechanism is obtained from the CGK formula as

$$f = 4(6-1) - 6 \times 3 = 2$$

However, the above result is wrong, for it predicts a too large dof. Indeed, the mechanism has one idle dof, as can be readily shown by means of a bond analysis: Let us

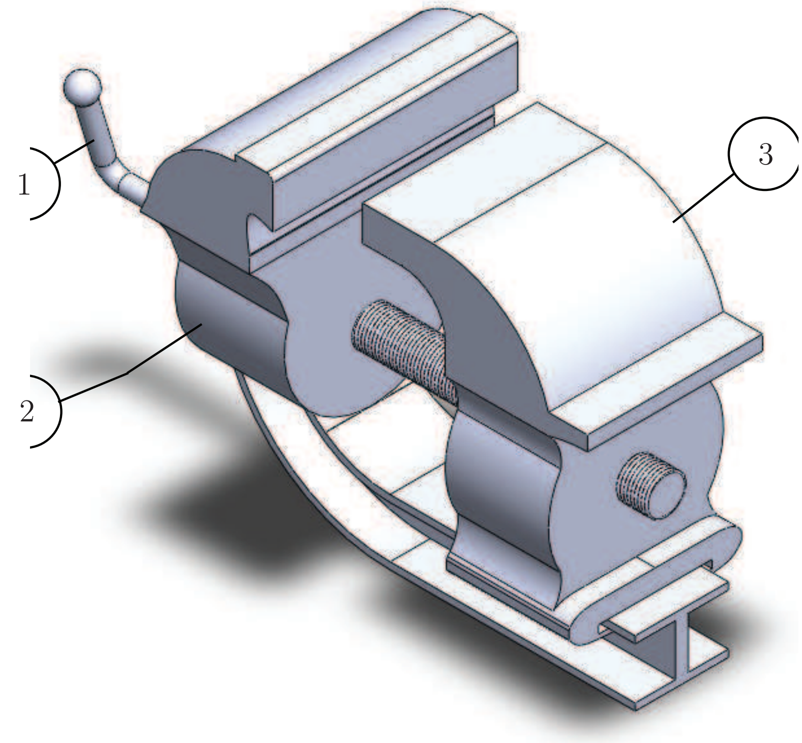


Figure 2.14: The well-known vise mechanism

compute $\dim[\mathcal{L}(1,5)]$:

$$\mathcal{L}(1,5) = \underbrace{\mathcal{L}(1,2) \bullet \mathcal{L}(2,3)}_{\mathcal{C}(\mathcal{A}_1)} \bullet \underbrace{\mathcal{L}(3,4) \bullet \mathcal{L}(4,5)}_{\mathcal{C}(\mathcal{A}_2)}$$

where $\mathcal{A}_1$ and $\mathcal{A}_2$ are axes parallel to vector $\mathbf{u}$ and pass through points $A$ and $B$, respectively, of Fig. 2.15. Now we find the above-mentioned idle dof. To this end, we compute $\dim[\mathcal{L}(1,5)]$, which may appear to be the sum of the dimensions of the two subgroups, $\mathcal{C}(\mathcal{A}_1)$ and $\mathcal{C}(\mathcal{A}_2)$. However, notice that these two subgroups include a common translation along $\mathbf{u}$, and hence, in computing the said dimension, care should be taken in not counting this translation twice. What this means is that the dimension of the intersection of the above two factors must be subtracted from the sum of their dimensions, i.e.,

$$\dim[\mathcal{L}(1,5)] = \dim[\mathcal{C}(\mathcal{A}_1)] + \dim[\mathcal{C}(\mathcal{A}_2)] - \dim[\mathcal{C}(\mathcal{A}_1) \cap \dim[\mathcal{C}(\mathcal{A}_2)] = 2 + 2 - 1 = 3$$

We have thus shown that the chain entails one idle dof. In order to obtain the correct dof of the chain from the generalized CGK formula, then, the total number $m$ of idle dof must be subtracted from the dof predicted by that formula, i.e.,

$$f = d_m(n-1) - \sum_{i=1}^{p} r_i - m \tag{2.13}$$

which can be fairly called the *Chebyshev-Grübler-Kutzbach-Hervé* formula. In the case at hand, $m = 1$, and hence, the dof of the chain of Fig. 2.15 is unity.

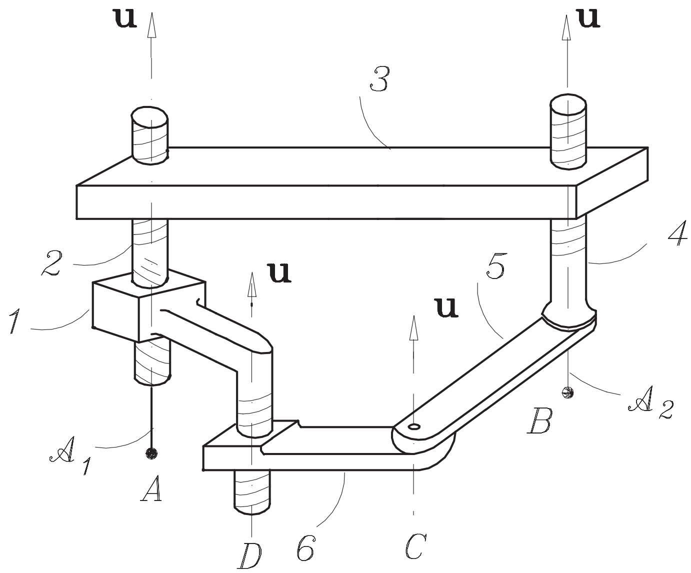


Figure 2.15: The HHHRRH mechanism

**Exercise 2.7.1** *A model of an automotive five-point suspension is included in Fig. 2.16* [3]*. This system is used to support and guide the front wheels upon turning and allowing for relative motion of each wheel with respect to the vehicle chassis. By moving a front wheel on a suspension of this kind while the vehicle is lifted from ground, it is possible to realize that the suspension has one single degree of freedom. Moreover, the mechanical system in question includes one fixed base, the chassis, one mobile platform, the metal frame on which the wheel is mounted, chassis and frame coupled by five links by means of* S *joints.*

*(i) Produce a graph representation of the suspension linkage;*

*(ii) Determine the degree of freedom of the linkage.*

### 2.7.2 Exceptional Chains

The Sarrus mechanism of Figs. 2.12 and 2.13 is an example of an exceptional chain. Indeed, all its links undergo motions of either one of two planar subgroups, $\mathcal{F}(\mathbf{u})$ and $\mathcal{F}(\mathbf{v})$. Moreover, the product of these two subgroups does not yield the group $\mathcal{D}$—notice that the linkage has two sets of R pairs, each parallel to a distinct unit vector, $\mathbf{u}$ or $\mathbf{v}$. The dof of this mechanism can still be found, but not with the aid of the CGK formula of eq.(2.12), for all its kinematic bonds do not belong to the same subgroup of $\mathcal{D}$. This dof is found, rather, as the dimension of the intersection of the two foregoing subgroups, i.e.,

$$f = \dim[\mathcal{F}(\mathbf{u}) \cap \mathcal{F}(\mathbf{v})] = \dim[\mathcal{P}(\mathbf{u} \times \mathbf{v})] = 1$$

[3] Taken from (Plecnik and McCarthy, 2013)

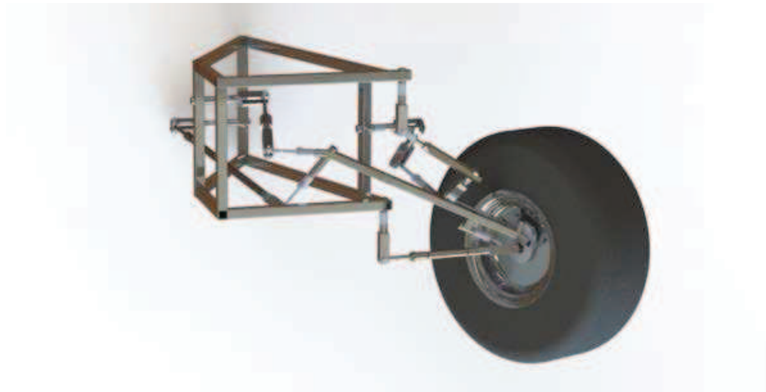

Figure 2.16: A five-point automotive suspension

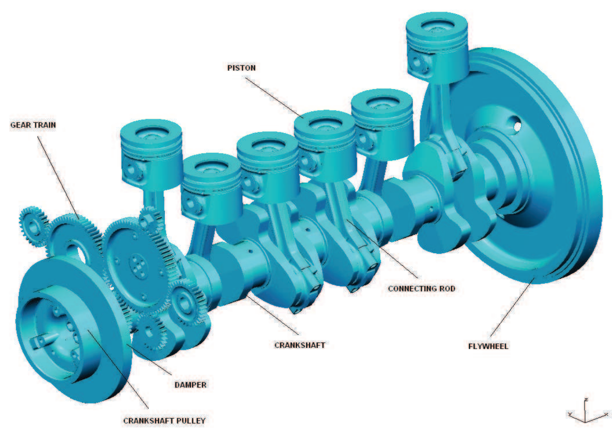


Figure 2.17: The slider-crank mechanism as a key component of an internal combustion engine: a power-generation system with six cylinders in line (courtesy of MMM International Motores, Campinas, Brazil)

Another example of exceptional chain is the familiar slider-crank mechanism of internal combustion engines and compressors, as shown in Fig. 2.17. It is customary to represent this mechanism as a planar RRRP mechanism. However, a close look at the coupling of the piston with its chamber reveals that this coupling is not via a prismatic, but rather via a cylindrical pair. It is thus apparent that the displacements of all the links lie not in one single subgroup of $\mathcal{D}$, but rather in a subset that can be decomposed into two kinematic bonds, which happen to be subgroups of $\mathcal{D}$, the $\mathcal{F}(\mathbf{e})$ subgroup of motions generated by the RRR subchain and the $\mathcal{C}(\mathcal{A})$ subgroup of the piston-chamber coupling C. Here, $\mathcal{A}$ is the axis of the cylindrical chamber and $\mathbf{e}$ is the unit vector parallel to the axes of the three R pairs. Apparently, the product of these two subgroups does not generate all of $\mathcal{D}$, for it is short of rotations about an axis normal to both $\mathbf{e}$ and $\mathcal{A}$. Nevertheless, the dof of this chain can be determined as the dimension of the intersection of the two subgroups, i.e.,

$$f = \dim[\mathcal{F}(\mathbf{e}) \cap \mathcal{C}(\mathcal{A})] = \dim[\mathcal{P}(\mathbf{u})] = 1, \quad \mathbf{u} \parallel \mathcal{A}$$

Now, why would such a simple planar mechanism—the slider-crank—as portrayed in elementary books on mechanisms, be built with a spatial structure? The answer to this question lies in the *assemblability* of the mechanism: a planar RRRP mechanism requires a highly accurate machining of the crankshaft, connecting rod, piston and chamber, in order to guarantee that the axes of the three R pairs are indeed parallel and that the axis of the cylindrical chamber is normal to the three R axes, which is by no means a simple task!

One more example of exceptional chain is the parallel robot of Fig. 2.18, consisting of four identical limbs that join a base $A_I A_{II} A_{III} A_{IV}$ with a moving plate $D_I D_{II} D_{III} D_{IV}$. Each limb, moreover, is a PRΠRR chain (Altuzarra et al., 2009).

The kinematic chain thus contains five joints per limb and 18 links: the base plate, the mobile plate and four intermediate links per limb. If the CGK formula is applied for the general kinematic chain, with $d_m = 6$, $l = 18$, $r_i = 5$, for $i = 1, \ldots, 18$, the dof $f$ thus resulting turns out to be

$$f = 6(18-1) - 20 \times 5 = 102 - 100 = 2$$

which is not what the authors claim, namely, four. In order to elucidate the apparent contradiction, we conduct below a group-theoretic analysis of the chain mobility: first, let $\mathcal{R}(P, \mathbf{e})$ denote the subgroup generated by a R joint of axis passing through point $P$ and parallel to the unit vector $\mathbf{e}$; then, let $\mathcal{L}_J$ denote the kinematic bond of the $J$th limb, which is the product of five simple bonds, each with a dimension equal to one, namely,

1. Either the prismatic subgroup $\mathcal{P}(\mathbf{i})$ of displacements parallel to $\mathbf{i}$, for $J = I, III$, or its counterpart $\mathcal{P}(\mathbf{j})$ of displacements parallel to $\mathbf{j}$, for $J = II, IV$;

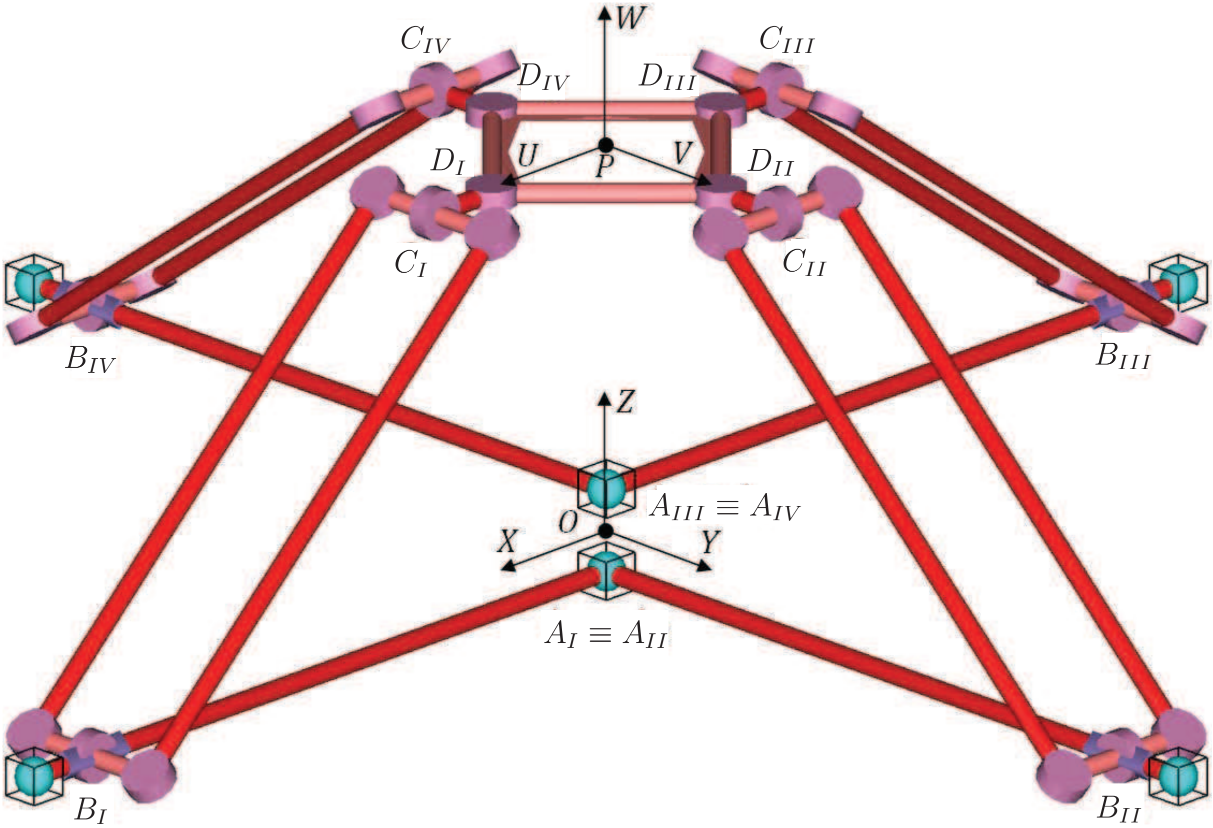


Figure 2.18: The Schönflies-motion generator developed at the University of the Basque Country, in Bilbao, Spain

2. the rotation subgroup $\mathcal{R}(B_J, \mathbf{j})$, of axis of rotation passing through point $B_J$ and parallel either to $\mathbf{j}$, for $J = I, III$, or its counterpart $\mathcal{R}(B_J, \mathbf{i})$, for $J = II, IV$;

3. the subset of displacements $\mathcal{D}_\Pi(\mathbf{n}_J)$ associated with the $\Pi$-joint, characterized by translations along circles of radius $\overline{B_J C_J}$ lying in the plane of the $J$th parallelogram, of normal $\mathbf{n}_J$;

4. the rotation subgroup $\mathcal{R}(C_J, \mathbf{j})$, of axis of rotation passing through point $C_J$ and parallel either to $\mathbf{j}$, for $J = I, III$ or to $\mathbf{i}$ for $J = II, IV$;

5. the rotation subgroup $\mathcal{R}(D_J, \mathbf{k})$ of axis of rotation passing through $D_J$ and parallel to $\mathbf{k}$.

Therefore,

$$\mathcal{L}_J = \underbrace{\mathcal{P}(\mathbf{i}) \bullet \mathcal{R}(B_J, \mathbf{j}) \bullet \mathcal{D}_\Pi(\mathbf{n}_J) \bullet \mathcal{R}(C_J, \mathbf{j})}_{\mathcal{X}(\mathbf{j})} \bullet \mathcal{R}(D_J, \mathbf{k}) = \mathcal{X}(\mathbf{j}) \bullet \mathcal{R}(D_J, \mathbf{k}), \quad J = I, III$$

Likewise,

$$\mathcal{L}_J = \mathcal{X}(\mathbf{i}) \bullet \mathcal{R}(D_J, \mathbf{k}), \quad J = II, IV$$

Notice that none of the four bonds derived above is a subgroup of $\mathcal{D}$, which disqualifies the multiloop kinematic chain from being trivial. However, notice also that

$$\mathcal{X}(\mathbf{j}) \bullet \mathcal{R}(D_J, \mathbf{k}) = \mathcal{X}(\mathbf{k}) \bullet \mathcal{R}(C_J, \mathbf{j}), \quad J = I, III$$

and

$$\mathcal{X}(\mathbf{i}) \bullet \mathcal{R}(D_J, \mathbf{k}) = \mathcal{X}(\mathbf{k}) \bullet \mathcal{R}(C_J, \mathbf{i}), \quad J = II, IV$$

Therefore,

$$\mathcal{L}_J \cap \mathcal{L}_K = \mathcal{X}(\mathbf{k}), \quad J,\, K = I, \ldots IV, \quad J \neq K$$

thereby proving that, indeed, the intersection of all limb bonds is a subgroup of $\mathcal{D}$, namely, the Schönflies subgroup $\mathcal{X}(\mathbf{k})$. The dof $f$ of the robot at hand is, thus,

$$f = \dim[\mathcal{X}(\mathbf{k})] = 4$$

and, according to Hervé's classification, the multiloop chain can be considered exceptional.

### 2.7.3 Paradoxical Chains

Examples of paradoxical chains are well documented in the literature (Bricard, 1927; Angeles, 1982). These include the *Bennett mechanism* and the *Bricard mechanism*, among others.

## 2.8 Applications to the Qualitative Synthesis of Robotic Architectures

The foregoing concepts are now applied to the *qualitative* synthesis of parallel robotic architectures. By qualitative we mean the determination of the topology of the kinematic chain, not including the corresponding dimensions. These dimensions are found at a later stage, by means of methods of *quantitative synthesis*, which Hartenberg and Denavit (1964) term dimensional synthesis, the subject of Chs. 3–5. The full determination of the kinematic chain, including dimensions, yields what is known as the *architecture* of the robotic system at hand.

### 2.8.1 The Synthesis of Robotic Architectures

The first robotic architecture with Π-joints was proposed by Clavel in what he called the *Delta Robot* (Clavel, 1988). The kinematic chain of this robot is displayed in Fig. 2.19. Delta is a generator of the $\mathcal{T}_3$ displacement subgroup; it is thus capable of three-dof translations.

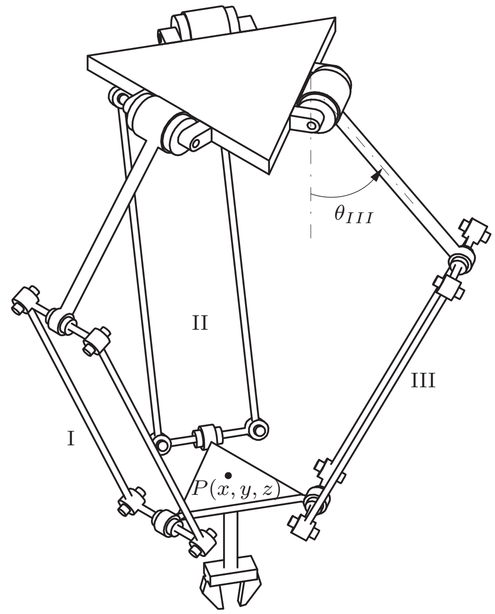


Figure 2.19: Kinematic chain of the Clavel Delta robot

The kinematic chain of the Delta robot is composed of two triangular plates, the top ($\mathcal{A}$) and the bottom ($\mathcal{B}$) plates. The top plate supports the three (direct-drive) motors, the bottom plate the gripper, and hence, constitutes the moving-platform (MP) of the robot. The MP is capable of translating in 3D space with respect to the upper plate, which is considered fixed. The two plates are coupled by means of three legs, each with a $\mathsf{RR\Pi R}$ chain.

To be true, the $\Pi$-joints of the actual Delta are not composed of $\mathsf{R}$ joints, but rather of *orientable pin joints*, equivalent to $\mathsf{S}$ joints. The reason is that providing parallelism between any pair of $\mathsf{R}$ axes is physically impossible. To allow for *assemblability*, then, a margin of manoeuvre must be provided.

While Clavel did not cite any group-theoretical reasoning behind his ingenious design, an analysis in this framework will readily explain the principle of operation of the robot. This analysis is conducted on the ideal kinematic chain displayed in Fig. 2.19.

The $i$th leg is a generator of the Schönflies $\mathcal{X}(\mathbf{e}_i)$ subgroup, with $\mathbf{e}_i$ denoting the unit vector parallel to the axis of the $i$th motor. That is, the $i$th leg generates a Schönflies subgroup of displacements comprising translations in 3D space and one rotation about an axis parallel to $\mathbf{e}_i$. The subset of EE displacements is thus the intersection of the three subgroups $\mathcal{X}(\mathbf{e}_i)$, for $i = 1, 2, 3$, i.e., the subgroup $\mathcal{T}_3$. Therefore, the EE is capable of pure translations in 3D space. This kinematic chain is, thus, of the exceptional type.

One second applications example is the microfinger of Japan's Mechanical Engineering Laboratory (MEL) at Tsukuba (Arai et al., 1996), as displayed in Fig. 2.20. In the MEL design, the authors use a structure consisting of two plates that translate with respect to each other by means of three legs coupling the plates. The $i$th leg entails a $\mathsf{R\Pi\Pi R}$ chain,

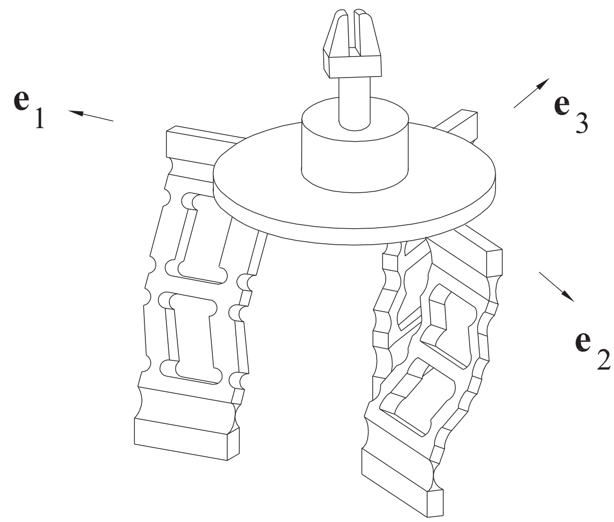


Figure 2.20: The MEL microfinger

shown in Fig. 2.21, that generates the Schönflies subgroup in the direction of a unit vector $\mathbf{e}_i$, for $i = 1, 2, 3$. The three unit vectors, moreover, are coplanar and make angles of 120° pairwise. The motion of the moving plate is thus the result of the intersection of these three subgroups, which is, in turn, the $\mathcal{T}_3$ subgroup. Moreover, the kinematic chain of each leg is made of an elastic material in one single piece, in order to allow for micrometric displacements.

Another example is the Y-Tristar robot, developed at Ecole Centrale de Paris by Hervé and Sparacino (1992). One more application of the same concepts is the four-dof SCARA-motion generator proposed by Angeles et al., (2000), and displayed in Fig. 2.22. This robot entails a kinematic chain of the $\mathsf{R\Pi R\Pi}$ type with two vertical revolutes and two $\Pi$-pairs lying in distinct, vertical planes. The Schönflies subgroup generated by this device is of vertical axis. While Delta and Y-Tristar are made up of Schönflies motion generators, the product of all these is the translation subgroup $\mathcal{T}_3$. A Schönflies motion generator with parallel architecture is possible, as shown in Fig. 2.23. This architecture is the result of coupling two identical Schönflies motion generators of the type displayed in Fig. 2.22, each generating the same Schönflies subgroup. As a result, the two-legged parallel robot generates the intersection of two identical subgroups, which is the same subgroup. Yet another application of the $\Pi$ pair is found in the four-degree-of-freedom parallel robot patented by Company et al. (2001), and now marketed by Adept Technology, Inc. under

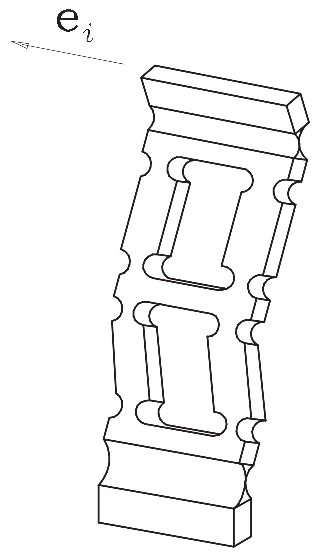


Figure 2.21: The $i$th leg of the MEL microfinger

the trade mark Quattro s650. A photograph of this robot is displayed in Fig. 2.24.

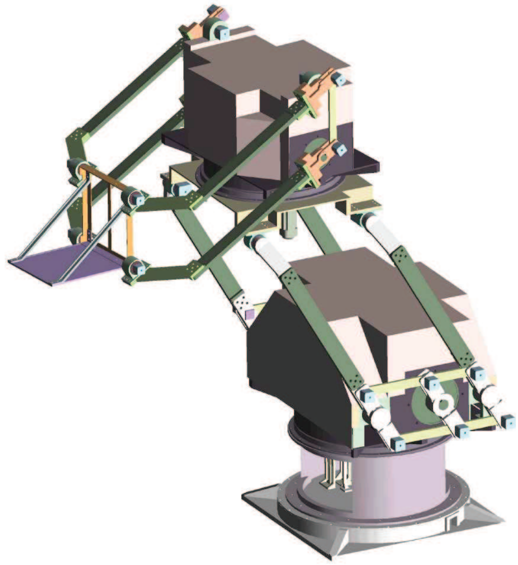

Figure 2.22: A serial-parallel Schönflies-motion generator with a RΠRΠ architecture

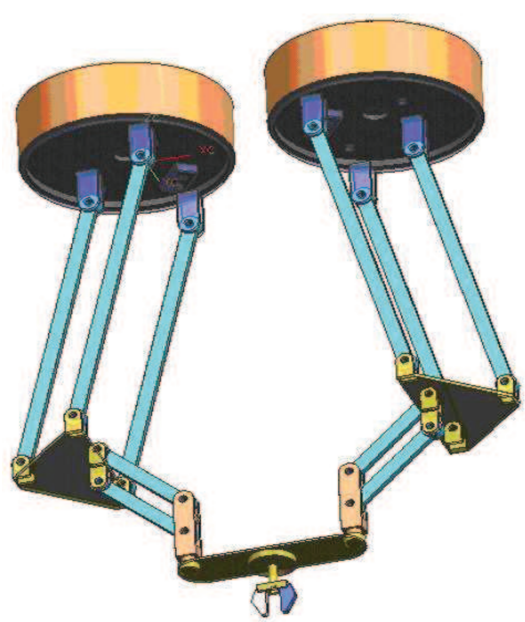

Figure 2.23: A parallel Schönflies–motion generator composed of two RΠRΠ legs

Figure 2.24: Adept Technology's Quattro robot, a parallel Schönflies–motion generator